Commun. Comput. Phys.
doi: 10.4208/cicp.OA-2018-0123

Vol. **28**, No. 1, pp. 498-517
July 2020

A Modified Multiple Matching Method Based on Equipoise Pseudomulti-Channel Filter and Huber Norm

Yinting Wu[1,*] and J. T. Wu[2]

[1] *School of Geological and Surveying & Mapping Engineering, Chang'an University, Xi'an 710064, P.R. China.*
[2] *School of CML Engineering & Architecture, Ningbo Institute of Technology, Zhejiang University, Ningbo 315100, P.R. China.*

Received 1 May 2018; Accepted (in revised version) 18 April 2019

Abstract. This study is aimed at improving multiple adaptive subtraction. We propose a modified pseudomulti-channel matching method based on the Huber norm, to adjust the matching differences on frequency and phase between the predicted multiples and original data. The second-order derivative of the predicted multiples is utilized to replace the derivative of its Hilbert transform. Due to the additional frequency term, this method can enhance the high-frequency component. We introduce 180° phase rotation of the multiple channels, which can decrease phase differences. The Huber norm interpolates between smooth L2 norm treatment of small residuals and robust L1 norm treatment of large residuals. This method can eliminate the restriction of large value conditions from the L2 norm and weaken the condition of orthogonality from the L1 norm. The applications of the Pluto and Delft models shows that compared with pseudomulti-channel matching filter, the main frequency is increased from 36 Hz to 38 Hz, and the primary reflection wave is more concentrated. The practical application of field data verifies the effectiveness of the proposed method.

AMS subject classifications: 74J25, 86A15, 86A22, 86A60

Key words: Multiple, adaptive matching filter, equipoise pseudomulti-channel, Huber norm, second-order derivative.

1 Introduction

In conventional seismic data processing, multiple waves are often regarded as interference, especially for marine seismic data, which have many multiple waves. Elimination of multiple waves is generally a critical step. There are two categories of elimination methods, one based on the difference between multiples and effective signals, and the

*Corresponding author. *Email addresses:* `wuyinting0215@163.com` (Y. Wu), `qingqing@163.com` (J. T. Wu)

other on wave equations. The latter utilizes a data-driven mode and needs little or no a prior information, such as the depth and velocity of the subsea. This type of method can achieve a good suppression effect and is currently a primary object of research. All of the current data-driven approaches, whether they use the feedback iterative method [1,2] or wavefield extrapolation method [3], have the two parts of prediction and subtraction. The predicted multiples are not likely to accurately coincide with the original data, including amplitude, arrival time, phase, and frequency. Therefore, a matching filter is required to achieve elimination when subtracting the predicted multiples from the original data.

There are many methods of adaptive matching filtering. The Wiener filter [4] can be implemented in both the time and frequency domains. The efficiency of the frequency Wiener filter suffers lower efficiency due to the associated nonlinear optimization problem. The time Wiener filter, by contrast, is simple and widely used. The pattern matching filter [5] requires predictability of events and is not ideal when the medium has strong lateral variations under complex conditions. The independent variable analysis method [6] is a kind of blind signal-separation technique that is only suitable when there is no time-shift between the multiple trace and original trace. The complex curvelet transform method [7] can correct the time-shift error well, but the processes of amplitude and phase correction are complicated.

We choose the time domain Wiener filter for its computational cost and effectiveness. The corresponding minimum-energy criteria can use different norms. For the L2 norm, it is fast to realize but sensitive to noise interference. Tarantola [8] proposed this norm's statistical interpretation on the interference signal. The L2 norm rests on two assumptions: multiples and primary reflection waves should have minimum energy differences, and they should be orthogonal. If not, there will be multiple solutions and the matching effect is neither satisfactory nor acceptable. Error measurement based on the L1 norm is common in geophysics. This norm has lower sensitivity to noise and is more robust than the L2 norm [9]. In addition, it has no restriction on large-value conditions, hence the energy difference between multiples and primary reflection waves should not be too large [10]. By adding a threshold parameter on the L1 norm and adopting a non-causal filter along the time axis, Xiong et al. [11] improved the matching effect and reduced the computation time. Unfortunately, with zero residual, the gradient of the L1 norm is singular and small errors are often amplified, so this criterion is often not applicable.

Considering the smoothness to small residuals of the L2 norm and the stability to large residuals of the L1 norm, the Huber norm is proposed [12]. This criterion is continuous at zero residual, uses the L1 norm for large residuals, and weights small residuals with the L2 norm. Ekblom and Madsen [13] deduced this optimization method. Guitton and William [14] used the Huber norm for velocity analysis and proved that it had higher stability than the least square method with damping. The complex Huber norm is applied to waveform inversion, and the gradient discretization formula of the Huber norm is deduced by Taeyoung et al. [15]. Its robustness to outliers and coherent noise is verified by Marmousi data. More recently, Li [16] calculated seismic curvature attributes based on this norm; as a result, not only is the fault boundary obtained but the fault property can be discriminated.

However, regardless of the norm used for the matching filter, there are orthogonality assumptions. This is often not the case for field seismic data, which makes the solution prone to instability and produces calculation error. Since multi-channel participation in matching can significantly reduce the orthogonal constraint between multiples and primary reflection waves, the multiple and its adjacent multiple channels are processed simultaneously [17]. Unlike the multi-channel filter, Monk [18] introduced derivative and Hilbert transform for multiple channels, and proposed the pseudomulti-channel adaptive matching method. This idea was applied in different ways by Wang [17] and Li et al. [19]. Liu [20] derived the solution through Z transformation. Li et al. [10] combined multi-channel and pseudomulti-channel matching methods, and proposed the equipoise pseudomulti-channel method. It is believed to achieve a better result than single- and multi-channel matching, through the Pluto model [21]. However, none of these methods considers frequency differences between multiples and primary reflection waves. Actually, due to two or more instances of wavelet convolution, the predicted multiples always have a lower frequency range and a descending dominated frequency [22]. The existence of frequency differences could influence the matching effect as much as other factors, so it also must be considered.

This study proposes an idea to improve and make use of the Huber norm and equipoise pseudomulti-channel filter, and verifies this modified method using synthetic models and field data. In the methodology, we utilize the second-order derivative of multiple channels to replace the corresponding derivative of the Hilbert transform. In this way, we produce phase rotation of 180° and an additional adjustment in the frequency for multiple traces. Multi-channel and pseudomulti-channel filters are combined in an equipoise pseudomulti-channel filter, which could weaken the orthogonality constraint. Finally, the Huber norm is chosen as the minimum-energy criterion to overcome the large-value constraint.

2 Methodology

Our proposed method has two parts: the first part involves the substitution of transformed channels in the pseudomulti-channel algorithm, and the second concerns the introduction and calculation of the Huber norm in multiple matching. Some improvements are proposed to the original method. First, the criteria of pseudomulti-channel matching filter and the Huber norm are discussed as below.

2.1 Pseudomulti-channel filter method

After multiples are predicted, they should be matched to corresponding signal in the original seismic records, since usually there are differences between them. This can be expressed as:

$$d_0(t)=d(t)-s(t)*m(t), \tag{2.1}$$

where $d(t)$ is the original channel, $d_0(t)$ is the primary-only record after multiple elimination, $m(t)$ is the predicted multiple channel, and $s(t)$ is the adaptive matching filter.

The expression in Eq. (2.1) is based on a single-channel matching filter. Since there is no horizontal restraint, it lacks horizontal bindings, and the orthogonality constraint leads to solution instability and errors [10]. To further improve the constraint conditions of orthogonality, pseudomulti-channel adaptive matching filter is introduced by Monk [18].

The pseudomulti-channel method takes advantage of the multiple channel and its mathematical adjoint channels as simultaneous input data [18]. It is expressed as:

$$d_0(t)=d(t)-\Big(s_1(t)*m(t)+s_2(t)*m'(t)+s_3(t)*m^H(t)+s_4(t)*m^{H'}(t)\Big), \tag{2.2}$$

where $m'(t)$ is the derivative of $m(t)$,$m^H(t)$ is the Hilbert transform of $m(t)$,$m'^H(t)$ is the derivative of $m^H(t)$, and $s_1(t)$,$s_2(t)$,$s_3(t)$, and $s_4(t)$ are the respective corresponding adaptive filters.

Eq. (2.2) shows that the pseudomulti-channel adaptive matching filter is performed using an original seismic channel, the corresponding predicted multiple channel and transformed multiple channels, including the derivative, Hilbert transform and the derivative of Hilbert transform to multiple channel. In this way, the waveform is corrected to a certain extent to bring the predicted multiple and original records to agreement.

Define the multiple channel as [18,20]:

$$m(t)=\int_0^{+\infty} A(\omega)\cos(\omega t+\theta(\omega))d\omega. \tag{2.3}$$

The corresponding analytical channel can be expressed as:

$$\begin{aligned} M(t)&=m(t)+im^H(t)\\ &=\int_0^{+\infty} A(\omega)e^{i[\omega t+\theta(\omega)]}d\omega. \end{aligned} \tag{2.4}$$

Based on the Euler formula, the real part of the above analytical channel can be written as:

$$m^*(t)=\int_0^{+\infty}\alpha(\omega)[\cos(\omega t+\theta(\omega))\cos(\varphi(\omega))-\sin(\omega(t-\tau(t))+\theta(\omega))\sin(\varphi(\omega))]d\omega, \tag{2.5}$$

where $\alpha(\omega)$ represents the amplitude, $\tau(t)$ is the time shift, and $\varphi(\omega)$ is the phase.

Assuming the time shift $\tau(t)$ is small, the variable in Eq. (2.5) can be rewritten as:

$$\begin{aligned} m^*(t)=\int_0^{+\infty}\Big[&A(\omega)\cos(\omega t+\theta(\omega))\frac{\alpha(\omega)\cos(\varphi(\omega))}{A(\omega)} \\ &-A(\omega)\cos'(\omega t+\theta(\omega))\frac{\alpha(\omega)\tau(t)\cos(\varphi(\omega))}{A(\omega)} \\ &+A(\omega)\sin(\omega t+\theta(\omega))\frac{\alpha(\omega)\sin(\varphi(\omega))}{A(\omega)} \\ &-A(\omega)\sin'(\omega t+\theta(\omega))\frac{\alpha(\omega)\tau(t)\sin(\varphi(\omega))}{A(\omega)}\Big]d\omega, \end{aligned} \tag{2.6}$$

where the derivative of the multiple channel is:

$$m'(t)=\int_0^{+\infty}A(\omega)\cos'(\omega t+\varphi(\omega))d\omega. \tag{2.7}$$

The Hilbert transform of the multiple channel is:

$$m^H(t)=\int_0^{+\infty}A(\omega)\sin(\omega t+\varphi(\omega))d\omega, \tag{2.8}$$

and the derivative of the Hilbert transform is:

$$m^{H'}(t)=\int_0^{+\infty}A(\omega)\sin'(at+\theta(\omega))d\omega. \tag{2.9}$$

Eq. (2.6) contains the multiple channels and the mathematical adjoint channels, which constitute the original pseudomulti-channel matching method.

2.2 Modified equipoise pseudomulti-channel filter method

The original pseudomulti-channel matching method makes use of the transformed multiple traces. Fig. 1 shows an input signal and its transformed signals. We can see that, compared with the input signal (blue thin solid line), the phase of its first derivative (green dashed line) changes 270°, and phase rotation of the Hilbert transform (red dotted line) trace is 90°. Unfortunately, the phase of the derivative of the Hilbert transform (purple dash-dot line) has no change, hence this transformed signal contributes little to waveform correction.

However, the phase of the second-order derivative rotates 180° (light blue thick line). Therefore, an improved pseudomulti-channel matching method is proposed on this basis, i.e., the second-order derivative replaces the derivative of its Hilbert transform. In other words, we utilize the first derivative, second-order derivative, and Hilbert transform of the predicted multiple channel to participate in the pseudomulti-channel calculation.

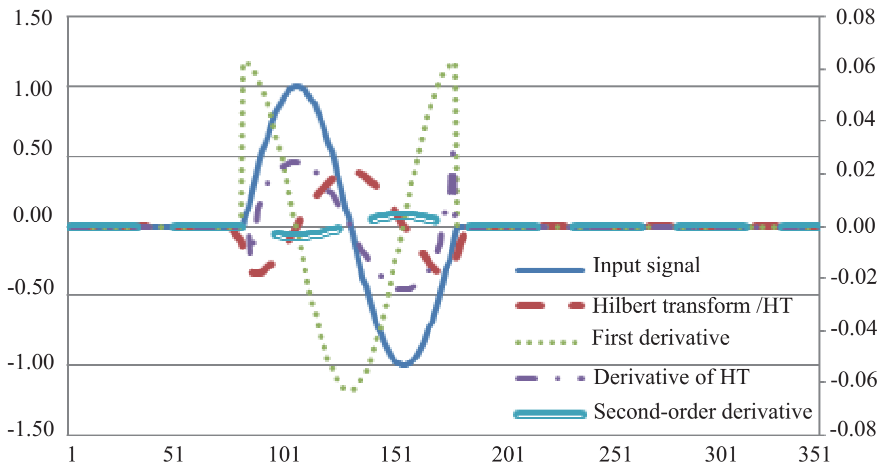

Figure 1: One signal and its transformed signals.

The second-order derivative channel in the time direction is:

$$m''(t)=\int_0^{+\infty}(-\omega)A(\omega)\sin'(\omega t+\theta(\omega))d\omega. \tag{2.10}$$

Comparing Eq. (2.10) to the derivative of the Hilbert transform channel (Eq. (2.9)), we can see that the second-order derivative not only has 180° phase rotation but also has a frequency-correction term.

Replacing the derivative of the Hilbert transform with the second-order derivative gives us the approximate formula:

$$\begin{aligned}m^*(t)=\int_0^{+\infty}\bigg[&A(\omega)\cos(\omega t+\theta(\omega))\frac{\alpha(\omega)\cos(\varphi(\omega))}{A(\omega)}\\&-A(\omega)\cos'(\omega t+\theta(\omega))\frac{\alpha(\omega)\tau(t)\cos(\varphi(\omega))}{A(\omega)}\\&+A(\omega)\sin(\omega t+\theta(\omega))\frac{\alpha(\omega)\sin(\varphi(\omega))}{A(\omega)}\\&-\frac{1}{(-\omega)}A(\omega)\sin'(\omega t+\theta(\omega))\frac{\alpha(\omega)\tau(t)\sin(\varphi(\omega))}{A(\omega)}\bigg]d\omega.\end{aligned} \tag{2.11}$$

According to Eq. (2.11), the fourth item has an extra factor of $\frac{1}{(-\omega)}$, compared with Eq. (2.6). Different amounts of correction are produced according to the frequency, which is believed to regulate frequency differences.

The introduction of 180° phase rotation and frequency-correction terms is thought to narrow the differences in phase and frequency between the original and predicted records. Also, the processed wavefield will be more concentrated and there will be less energy leakage or residue compared to the original method.

However, although the transformed channels can modify waveform correction, orthogonality condition still must be met. Since the non-Gaussian nature of a single channel is weak, the decomposition of multiples and primary reflection waves is not good enough. For further improvement, multi-channel is combined with pseudomulti-channel, which creates an equipoise pseudomulti-channel matching method [19]. The significance of equalization lies in the statistical average effect. We take advantage of diverse channels to enhance the non-Gaussian property, thereby improving the limit for orthogonality. This balanced idea assumes that the multiple channels have the same wavelet within the calculated time window, which is not very harsh.

Set the number of channels involved as k. Then the filtering progress of our modified equipoise pseudomulti-channel filter method can be expressed as:

$$d_{oi}(t)=d_i(t)-\Big[s_{1i}(t)*m_i(t)+s_{2i}(t)*m_i'(t)+s_{3i}(t)*m_i^H(t)+s_{4i}(t)*m_i''(t)\Big], \tag{2.12}$$

where $m_i(t)$, $m_i'(t)$, $m_i^H(t)$, and $m_i'(t)$ are respectively the ith multiple channel and its corresponding transformed channels, $d_i(t)$ is the ith original channel, $d_{0i}(t)$ is the ith primary reflection channel, and $s_{1i}(t)$, $s_{2i}(t)$, $s_{3i}(t)$, and $s_{4i}(t)$ are the corresponding filters.

2.3 Huber norm

The Huber norm is a combination of the L2 and L1 norms, we will review these two norms first. In the discussion of the feedback iterative method, Verschuur et al. [2] proposed the single-channel L2 norm in the frequency domain [1]. Some researchers (Li et al. [10]) have adopted the single-channel L2 norm in the time domain [2]. The adaptive filter of the L2 norm in the time domain can be obtained as:

$$s(t): \quad \min\|d(t)-s(t)*m(t)\|_2. \tag{2.13}$$

The least squares problem is settled by differentiating $s(t)$ and setting it to zero:

$$M^T(d-Ms)=0, \tag{2.14}$$

where $M((2n-1)\times(n-1))$ is the matrix form of multiple records:

$$M=\begin{pmatrix} m(1) & 0 & 0 & 0 \\ m(2) & m(1) & 0 & 0 \\ \vdots & m(2) & \ddots & \vdots \\ m(n-1) & \ddots & \ddots & m(1) \\ m(n) & m(n-1) & \ddots & m(2) \\ 0 & m(n) & \ddots & \vdots \\ \vdots & \vdots & \ddots & m(n-1) \\ 0 & 0 & 0 & m(n) \end{pmatrix}. \tag{2.15}$$

M^T is the transposition of M, Eq. (2.14) can be expressed as:

$$M^T M s = M^T d. \tag{2.16}$$

Solution of s is given by:

$$s = \left(M^T M\right)^{-1} M^T d. \tag{2.17}$$

The numerator $M^T d$ is the delay cross-correlation of multiple model $m(t)$ and seismic record $d(t)$; the denominator $M^T M$ is the self-correlation of multiple model $m(t)$. $M^T M$ is a symmetric Toeplitz matrix, so the linear equation can be quickly solved by the Levinson method.

When determining the filter solution, a seismic channel from the original record and its corresponding multiple record are input to perform the matching. Therefore, this method is known as single-channel adaptive matched filtering. When there is only amplitude scale difference between the predicted multiple and the original data, the matching filter can obtain better results [23].

To obtain the solution of the $L2$ norm, it must satisfy the following condition [10]:

$$m(t) \cdot d_0(t) = 0. \tag{2.18}$$

That is, the primary reflections and multiples must satisfy orthogonality condition. In theory, this method requires that no intersection, overlap, or superposition exist between primaries and multiples. However, this is very difficult to satisfy with the actual data, which is one of its shortcomings.

The matching-filter method based on the $L2$ norm also requires that the energy of primary reflections is not much larger than that of multiples, i.e., there is a large-value condition in addition to the orthogonality requirement. Otherwise, if multiples in the seismic records are much weaker than the effective waves near them, the solution of adaptive filter $s(t)$ is not accurate, and there will be errors.

To avoid the large-value condition, Guitton and Verschuur [24] proposed a least adaptive matching filter method based on the single-channel $L1$ norm. Taylor and Banks [25] proposed this $L1$ norm method for deconvolution and matching filtering because its output is sparser.

The $L1$ norm matching filter is based on the minimum $L1$ norm of the target function. It is derived from the adaptive filter by minimizing the following objective function:

$$s(t): \quad \min \| d(t) - s(t) * m(t) \|_1. \tag{2.19}$$

The contrast analysis on the $L2$ and $L1$ norms is as follows. It is generally believed that the filter method with the $L2$ norm minimum principle tends to decrease the amplitude of output data as much as possible, which achieves a certain de-noising. This method ignores small events because of smaller energy value. However, when a primary reflection event has strong energy and is close to a predictive multiple, the filtering factor

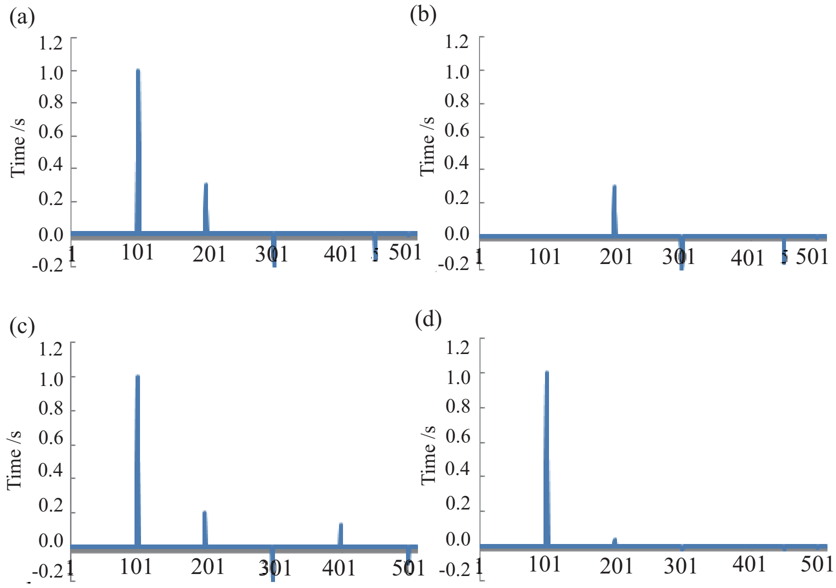

Figure 2: The original signal and its multiple matching result: (a) the original signal; (b) its predicted multiple; (c) the signal after $L2$ norm matching filter; (d) the signal after $L1$ norm matching filter.

will weaken its energy, but for the $L1$ norm matching filter, the sum of the absolute value of energy is smaller than that of the $L2$ norm. This can be verified by the simple model results shown in Fig. 2.

The Huber norm was proposed by Huber in 1973 as an error measure; it is a hybrid of the $L1$ and $L2$ norms. It treats small residuals with the $L2$ norm and large residuals with the $L1$ norm:

$$M_\varepsilon(r)=\begin{cases} \frac{r^2}{2\varepsilon}, & 0\le|r|\le\varepsilon, \\ |r|-\frac{\varepsilon}{2}, & \varepsilon<|r|, \end{cases} \tag{2.20}$$

where r is the residual and ε is the threshold between the $L1$ and $L2$ norms, or can also be called as the priori value. The implementation is shown in Fig. 3. The (black) solid line corresponds to the $L1$ norm and the (red) dotted line to the $L2$ norm.

2.4 Modified method based on equipoise pseudomulti-channel filter and Huber norm

For the prediction and subtraction of multiple elimination, the Huber function is established to optimize the process:

$$\min: \quad |d(t)-s(t)*m(t)|_{Huber}=|r|_{Huber}=\sum_{i=1}^{N}\left(\sqrt{1+(r_i/\varepsilon)^2}-1\right)=\sum_{i=1}^{N}M_\varepsilon(r_i), \tag{2.21}$$

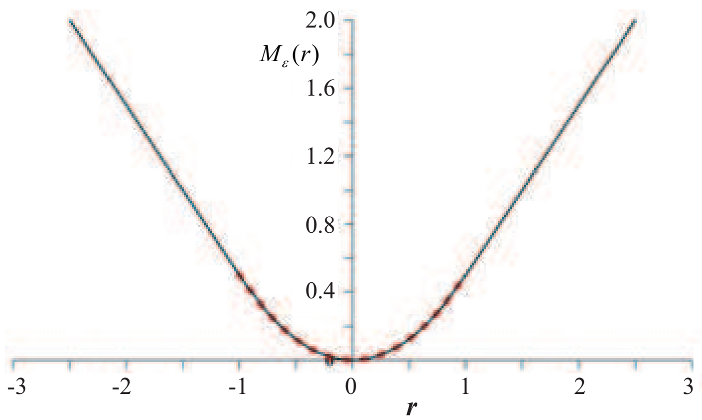

Figure 3: Huber norm (here, $\varepsilon=1$, with black solid line as $L1$ norm and red dotted line as $L2$ norm).

where r_i $(i=1,2,\cdots N)$ is the residual representing the ith primary reflection data element after multiple elimination, N is the total number of discrete points, and ε usually can be taken as $\frac{\max|d|}{100}$.

From Eqs. (2.20) and (2.21) we can see that when the difference r_i between the primary and the multiple is small and less than a threshold ε, the $L2$ norm is taken as the mean square; otherwise the $L1$ norm taking into action as a median filter. Therefore, there is no large-value constraint on the Huber norm. Apply the equipoise pseudomulti-channel matching method based on the Huber norm with Eq. (2.12), then the objective function can be written as:

$$\min: \quad \Big| d_i(t) - \Big[s_{1i}(t)*m_i(t) + s_{2i}(t)*m_i'(t) + s_{3i}(t)*m_i^H(t) + s_{4i}(t)*m_i''(t) \Big] \Big|_{Huber}. \tag{2.22}$$

To facilitate the operation, the above formula is written in matrix form, and during the solution for the Huber norm, a weighted matrix W_i is introduced, and we can write as:

$$\begin{aligned} \min: \quad & \sum_{i=1}^{k} \Big| d_i(t) - \Big(M_i s_{1i} + M_i' s_{2i} + M_i^H s_{3i} + M_i'' s_{4i} \Big) \Big|_{Huber} \\ = & \sum_{i=1}^{k} \Big\| W_i \Big(d_i(t) - (M_i s_{1i} + M_i' s_{2i} + M_i^H s_{3i} + M_i'' s_{4i}) \Big) \Big\|_2, \end{aligned} \tag{2.23}$$

where $W_i = \mathrm{diag}\Big(\frac{1}{(1+\frac{r_i^2}{\varepsilon^2})^{1/4}}\Big)$. According to our experience, a desirable result can be obtained when setting the number of input channels k to 3 or 5.

Let these partial derivatives for s_i be zero, and the Levinson method is employed:

$$\begin{aligned}&\Big[M_1^TW_1^TW_1^T(d_1-M_1s_1)+M_2^TW_2^TW_2^T(d_2-M_2s_2)+\cdots+M_k^TW_k^TW_k^T(d_k-M_ks_k)\Big]\\&+\Big[M_1'^TW_1^TW_1^T(d_1-M_1's_1)+M_2'^TW_2^TW_2^T(d_2-M_2's_2)+\cdots+M_k'^TW_k^TW_k^T(d_k-M_k's_k)\Big]\\&+\Big[M_1^{HT}W_1^TW_1^T(d_1-M_1s_1)+M_2^{HT}W_2^TW_2^T(d_2-M_2^Hs_2)+\cdots+M_k^HW_k^TW_k^T(d_k-M_k^Hs_k)\Big]\\&+\Big[M_1''^TW_1^TW_1^T(d_1-M_1''s_1)+M_2''^TW_2^TW_2^T(d_2-M_2''s_2)+\cdots+M_k''^TW_k^TW_k^T(d_k-M_k''s_k)\Big]=0.\end{aligned} \tag{2.24}$$

The orthogonal requirement of Eq. (2.18) should be changed to:

$$\begin{aligned}&(m_{01}\cdot d_{01}+m_{02}\cdot d_{02}+\cdots+m_{0k}\cdot d_{0k})+(m_{01}'\cdot d_{01}+m_{02}'\cdot d_{02}+\cdots+m_{0k}'\cdot d_{0k})\\&+(m_{01}^H\cdot d_{01}+m_{02}^H\cdot d_{02}+\cdots+m_{0k}^H\cdot d_{0k})+(m_{01}''\cdot d_{01}+m_{02}''\cdot d_{02}+\cdots+m_{0k}''\cdot d_{0k})=0,\end{aligned} \tag{2.25}$$

where m_{0i}, m_{0i}', m_{0i}^H, and m_{0i}'' $(i=1,2,\cdots,k)$ are respectively the ith record gained by filtering its corresponding first derivative, its Hilbert transform, and the second-order derivative channels; and d_{0i} is the primary reflection record after filtering.

This means that the sum of inner products, including the multiple and primary reflection channels, the transformed multiple channels, and the primary reflection channel are zero. Compared to the orthogonal of multiples and primary reflection waves, the demand is weakened substantially.

For the solution, the quasi-Newton method [26], or the direct iteration method [19] can be used. Taking into account the convergence rate, the latter is chosen in this research. The specific process is as follows. Set the original value of the matching filter to $s=(1,0,\cdots,0)^T$ and substitute this into the objective function. Next, the weighted matrix is further calculated through the resulting initial residual (the primary reflection data) and then substituted into the equation set to update s. Step iterations are conducted until satisfactory results are obtained. In our test example, five times seem fine.

3 Application of synthetic dataset

To verify the effectiveness, theoretical data including the Delft and Pluto models were processed and utilized to show the contrast before and after multiple elimination.

3.1 Delft model

The Delft model of a complex underground structure was designed by the SMAART organization, and it is a test platform to verify the multiple-suppression algorithm. It has very developed multiples. Specifically, it contains the seabed with large fluctuation, reflection interface with a great reflection coefficient, and a deep complex salt-dome structure. There are four horizontal interfaces in this model. The velocity of the third layer

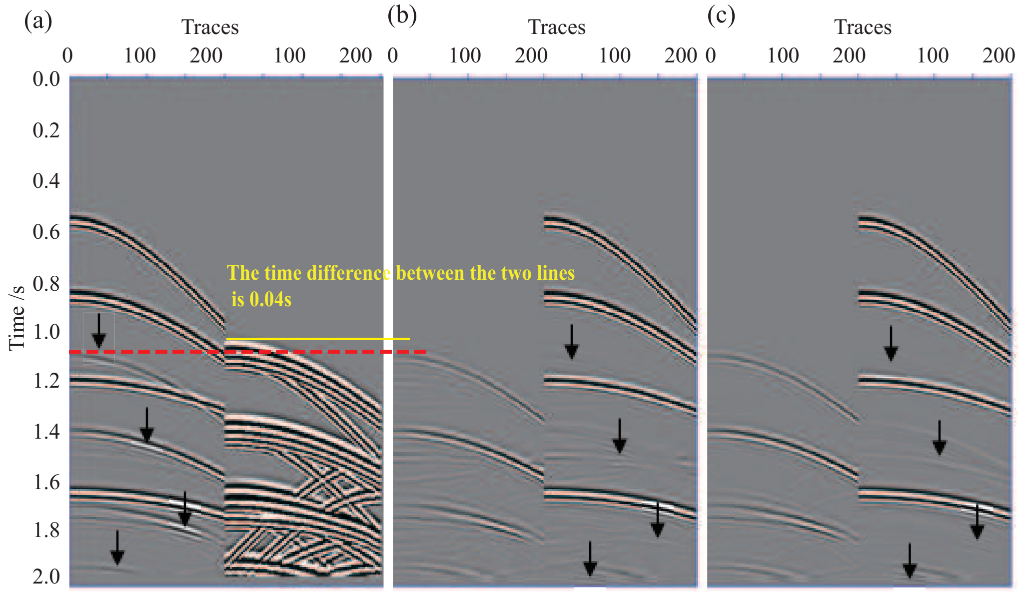

Figure 4: Comparison of pseudo-multichannel filter and the modified filter for Delft model: (a) original record (at left) and predicted multiple record (at right); (b) multiple record (at left) and primary reflection record (at right) after pseudomulti-channel filter; (c) multiple record (at left) and primary reflection record (at right) after the modified filter.

is 3,000 m/s, while that of the second and fourth layers is 2,000 m/s, so there is a large velocity contrast. The model data are calculated with the finite difference algorithm, as shown in Fig. 4(a), where some strong surface-related multiples are indicated by arrows. There are 200 receivers for each shot.

It can be seen from the original record at the left of Fig. 4(a) that the waveform has a longer duration and contains two side lobes; the energy of primary reflection from four interfaces is very strong; surface multiples appear, but with relatively weak energy, and multiples and primary reflection waves partially overlap; and there is a weak event which is an internal multiple with the initial arrival near 1.5 s. The right part of Fig. 4(a) shows the surface multiple model predicted by the iterative feedback method SRME (surface related multiple elimination). It can be seen that multiple waves exist in each reflection interface, but their energy is very strong, and there is a certain time difference of 0.04 s (marked with the two dotted lines) compared with the original multiple record.

Figs. 4(b) and 4(c) show the records after multiple matching (at left) and multiple suppression (at right) by the pseudomulti-channel Huber norm filter and the modified filter, respectively. The comparison results show that from the modified equipoise pseudomulti-channel filter, the multiple suppression is more complete, with less noise and fewer multiples. Arrows mark the locations of multiple waves.

3.2 Pluto model

We compared our proposed method with the original pseudomulti-channel matching method. The two methods were applied to the released Pluto data. Take the 183rd shot as an example for analysis. This shot has 360 traces with interval of 25 m. The results are shown in Fig. 5, where Fig. 5(a) shows the original record and Fig. 5(b) shows the multiple record predicted by the SRME method. Intuitively, the energy of multiples is strong and there are still arrival time differences. Figs. 5(c) and 5(d) display the spectral analysis for the same selected traces from the original and predicted multiple records, respectively. We can see that the original one has dominant frequency of 40 Hz and is with the range of $15-80$ Hz, while the corresponding values for the multiple are 33 Hz and $20-65$ Hz. According to the contrasts, the predicted multiple has a narrower range of frequency and lower main frequency. This is because the prediction process entails the convolution of more than one wavelet, so that the energy of the high-frequency component from the

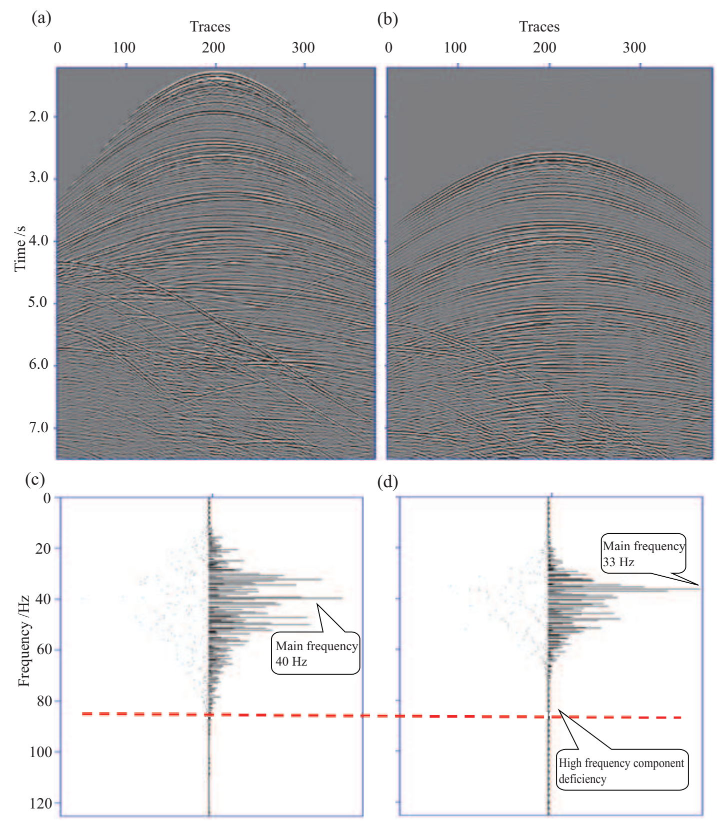

Figure 5: The 183rd shot of the Pluto model, predicted multiple records, and their spectrum analysis: (a) the 183rd original shot; (b) predicted multiple record; (c) spectrum analysis of the original shot record; (d) spectrum analysis of the predicted multiple record.

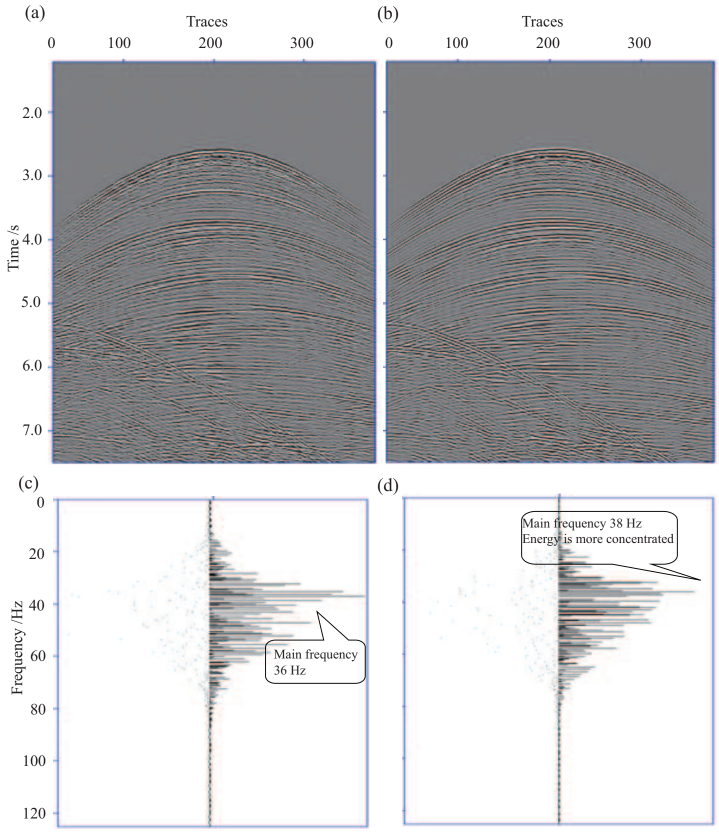

Figure 6: Matched multiple records and their spectrum analysis after pseudomulti-channel filter and the modified filter: (a) multiple record after pseudomulti-channel filter; (b) multiple record after the modified filter; (c) spectrum analysis after pseudomulti-channel filter; (d) spectrum analysis after the modified filter.

predicted multiple declines, and it has a narrower frequency band than the actual wave field.

The multiple records for the 183rd shot after the matching filter are displayed in Figs. 6(a) and 6(b), and the corresponding spectral analysis results are shown in Figs. 6(c) and 6(d). It can be concluded that after the adaptive matching of the pseudomulti-channel filter, the frequency components of multiple records are enriched, and the main frequency increases from 33 Hz to 36 Hz. In contrast, after our modified method, the energy is more concentrated and the main frequency increases to 38 Hz.

The analysis results [seen in Figs. 7(a) and 7(b)] of the primary reflection spectrum from matching subtraction between the two methods show that the main frequency after suppressing multiple waves by the pseudomulti-channel filter is 40 Hz, and the main energy is in the range of $30-60$ Hz. However, in this band, the energy appears to be divided into three distinct segments, and the energy is not concentrated. The main fre-

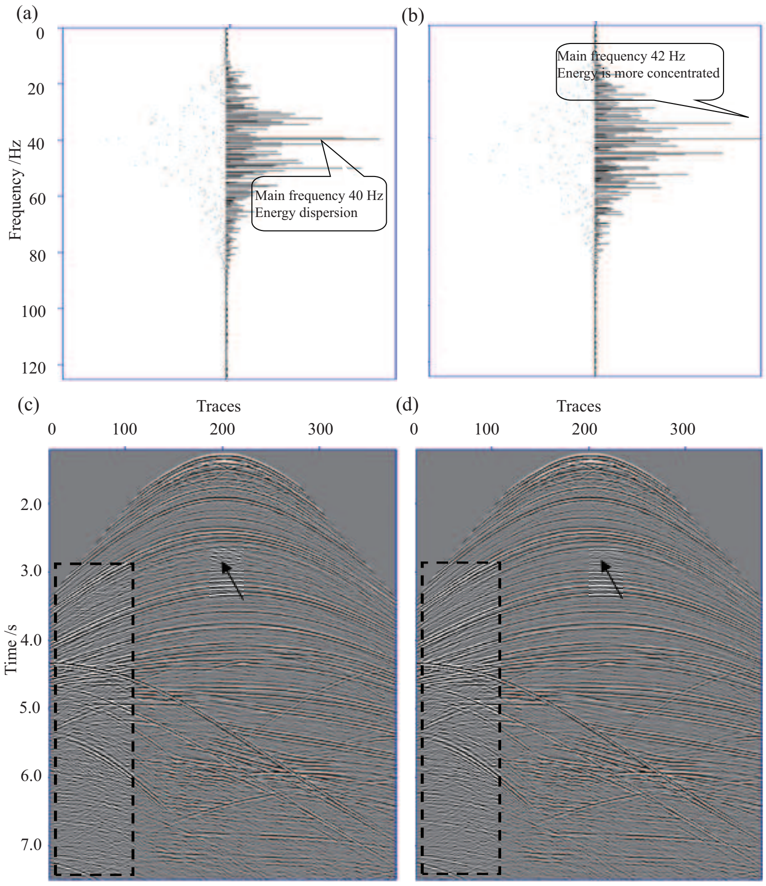

Figure 7: Primary reflection records after pseudomulti-channel matching suppression and our modified method: (a) spectrum analysis of primary reflection after pseudomulti-channel filter; (b) spectrum analysis of primary reflection after modified filter; (c) primary reflection record after pseudomulti-channel filter; (d) primary reflection record after modified filter.

quency of primary reflection energy obtained by the modified filter is 42 Hz, and the energy distribution is more concentrated at $30-65$ Hz. Figs. 7(c) and 7(d) show the filtering results before and after the improvement of the equipoise pseudomulti-channel Huber norm. In the event indicated by arrows, the improved filter enables the prediction of both the phase difference and frequency difference, the surface-related multiple is thoroughly suppressed, the primary reflection is well preserved, and the event is continuous, smooth, and clear. In the dashed frame, there is less multiple residue but stronger primary reflection energy with our improved method.

Figs. 8(a) and 8(b) show the multiple stack sections obtained from two matching filter methods. Comparing the two sections, especially the regions indicated by arrows, the multiple event energy based on the modified method is concentrated and coherent, with little interference. Figs. 8(c) and 8(d) show the stack sections after multiple suppres-

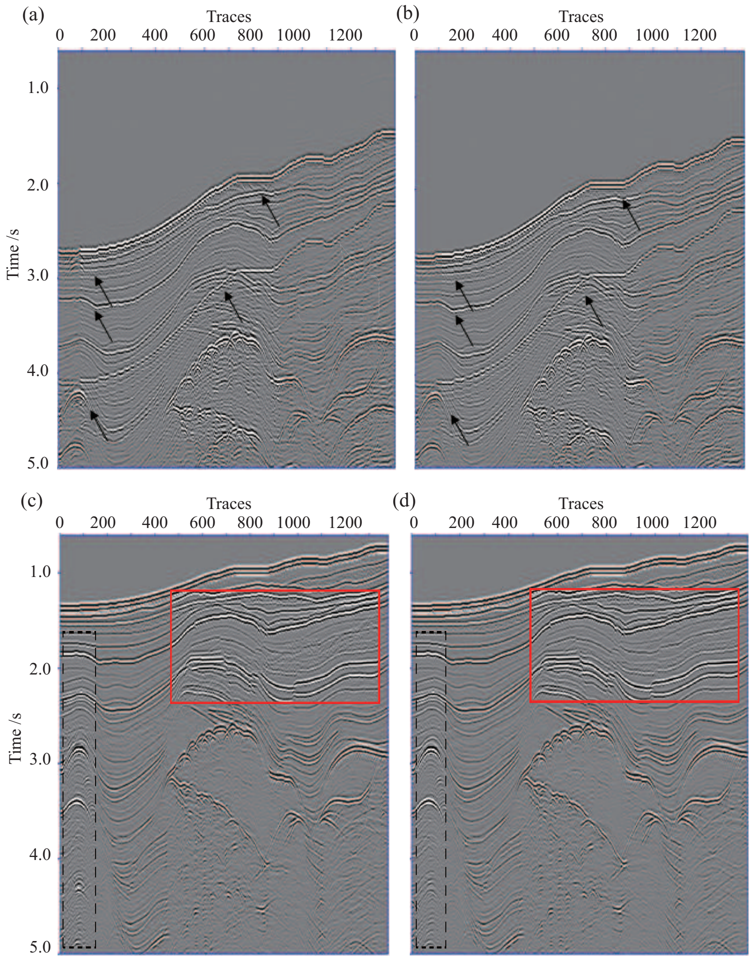

Figure 8: Stack section after multiples suppressed with pseudomulti-channel matching filter and the modified filter: (a) stack section of multiple based on pseudomulti-channel matching filter; (b) stack section of multiple based on the modified filter; (c) stack section after multiples suppressed based on pseudomulti-channel matching filter; (d) stack section after multiples suppressed.

sion. Comparing the red solid rectangular calibration sections at the upper-right corner of Figs. 8(c) and 8(d), with the modified matching filter method, there are fewer relative remnants of first-order multiples on the seabed, and there is no damage to the effective wave. In the black dotted rectangular calibration sections at the lower-left corner of Figs. 8(c) and 8(d), the new filter makes the interference smaller, and the multiple suppression is complete. It can be concluded from the above results that the modified matching method can achieve a better multiple suppression effect after subtraction, because it can well match the phase and frequency differences between the original multiples and predicted multiples.

4 Field data application

A marine seismic dataset was selected to carry out multiple suppression processing. Fig. 9(a) shows an original single shot record with 240 channels, where some strong surface-related multiples are indicated by arrows. Fig. 9(b) shows the multiple records predicted by the SRME method. In the prediction process, Radon transform is used to

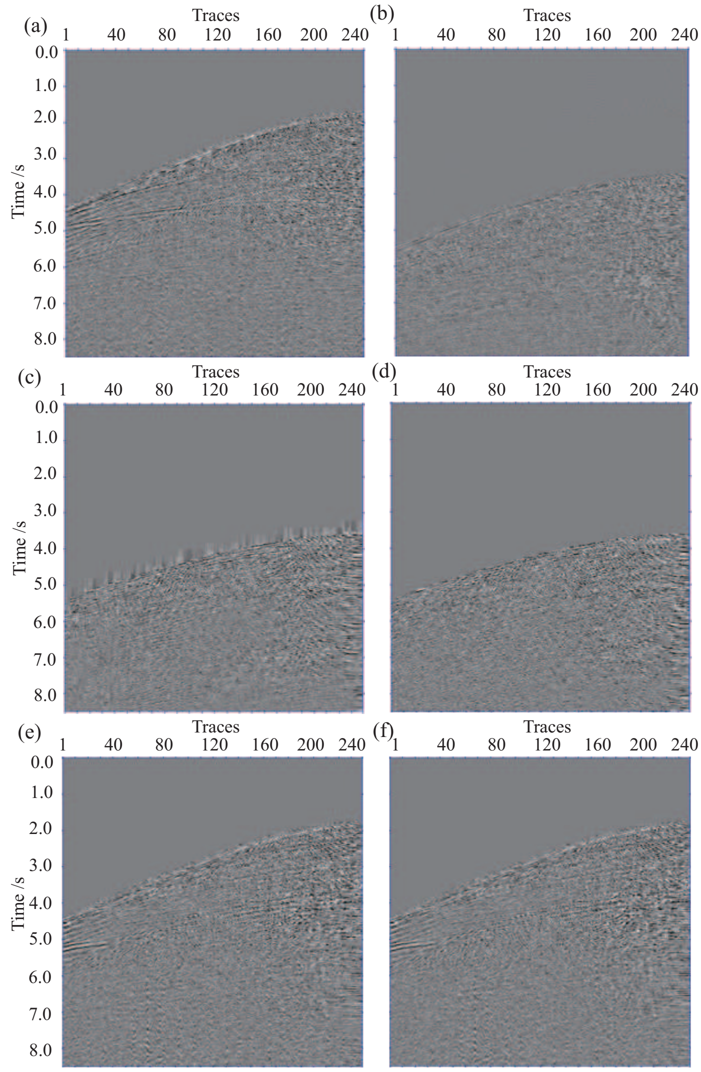

Figure 9: The field data, corresponding predicted multiple records, and primary records after multiple suppression: (a) the original shot record; (b) predicted multiple record; (c) multiple record with original pseudomulti-channel filter; (d) multiple record with the modified filter; (e) primary reflection record after multiple suppression with pseudomulti-channel filter; (f) primary reflection record after multiple suppression with the modified filter.

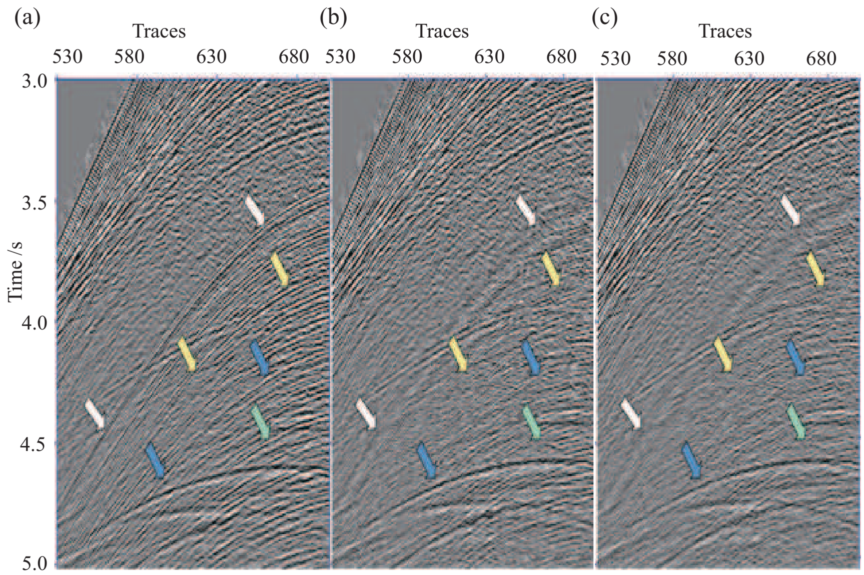

Figure 10: Partial enlarged view of the field data (a) and its corresponding primary reflection data with pseudomulti-channel matching filter (b) and with the modified filter (c).

carry out the near offset extrapolation. The predicted multiples are consistent with the original records, but errors exist in the amplitude and phase. Figs. 9(c) and 9(d) show the corresponding multiple records after matching by the original pseudomulti-channel filter and the modified filter, respectively. Due to noise and other interference in the field data, interference is generated in the multiple records. After the modified equipoise pseudomulti-channel Huber norm matching, it can be seen that the multiple events are more continuous and distinct. The two matched multiple records are reduced from the original records, and the obtained effective records are shown in Figs. 9(e) and 9(f). On the whole, the surface-related multiple energy is greatly reduced. To make a better comparison, a partial magnification is shown in Fig. 10. The former is the matching suppression result with the original filter method, and the latter is the result with the modified method. Arrows mark the locations of multiples.

5 Conclusions and discussion

This study proposed an improved filter based on equipoise pseudomulti-channel matching and the Huber norm. With the second-order derivative channel of multiple records replacing the derivative of Hilbert transform, we introduce the phase correction of 180° and the frequency additional term. From the application and comparison to synthetic and field data, this improvement can be believed partly promote the matching effect.

A large amount of actual data, especially in actual complex underground structures, show that this method is more effective than the conventional filtering method, such as in the situation of reverse velocity. However, for data with poor original quality or information, including low signal-to-noise ratio and irregular observation systems, this method cannot completely suppress multiples, and there may be obvious residual multiples or damaged primary reflection waves. In addition, the predicted multiples as the input data may have errors themselves, which will bring more errors to the subsequent steps of multiple-matching and suppression.

It is worth mentioning that besides the time and frequency domain, the matching subtraction for primary reflection and multiples can be done in other domains, such as the curvelet domain [27,28]. In short, whether it is based on the L1 or L2 norm, and whether it is in the time domain, frequency domain, or another domain, various matching methods are proposed and are still evolving and improving. It is wise to recognize and master the advantages and disadvantages of different methods, and to choose appropriate matching methods for different data characteristics.

Acknowledgments

This work is supported by the Fundamental Research Funds for the Central Universities (Grant No. 300102268212), Postdoctoral Science Foundation (2013M540756, 2014T70925), and Shaanxi Natural Science Foundation (2014JQ2-4019). The authors wish to acknowledge the support and contributions of the project sponsors, other participating institutions, and their personnel.

References

[1] D. J. Verschuur, A. J. Berkhout, and C. P. Wapenaar, Adaptive surface-related multiple elimination, Geophys., 57(9) (1992), 1166-1177.

[2] D. J. Verschuur and A. J. Berkhout, Estimation of multiple scattering by iterative inversion, Part II: Practical aspects and examples, Geophys., 62(5) (1997), 1596-1611.

[3] J. W. Wiggins, Attenuation of complex water bottom multiples by wave equation based prediction and subtraction, Geophys., 53(12) (1988), 1527-1539.

[4] N. Wiener, Extrapolation, interpolation, and smoothing of stationary time series, New York, 1949.

[5] S. Spitz, Pattern recognition, spatial predictability and subtraction of multiple events, The Leading Edge, (1999), 55-58.

[6] W. K. Lu, Y. Luo, B. Zhao, and Z. P. Qian, Adaptive multiple wave subtraction using independent component analysis,Chinese J. Geophys., 47(5) (2004), 886-891.

[7] L. Q. Dong, P. M. Li, K. Zhang, C. H. Wang, Y. Zhu, and Z. Wang, Primary and multiple separation method based on complex curvelet transform, Chinese J. Geophys., 58(10) (2015), 3783-3790.

[8] A. Tarantola, Inverse Problem Theory and Methods for Model Parameter Estimation, USA: Society for Industrial and Applied Mathematics, 1987.

[9] J. F. Claerbout and F. Muir, Robust modeling with erratic data, Geophys., 38 (1973), 826-844.

[10] X. C. Li, Y. K. Liu, X. Chang, and P. Li, The adaptive subtraction of multiple using the equipoise multichannel L1 norm matching, Chinese J. Geophys., 53(4) (2010), 963-973.

[11] F. S. Xiong, X. W. Huang, D. Zhang, R. X. Li, and P. Wang, Adaptive multiple subtraction method based on hybrid L1/L2 norm, Geophys. Geochem. Explor., 38(5) (2014), 996-1002.

[12] P. J. Huber, Robust regression: asymptotics, conjectures, and Monte Carlo. Ann. Statist., 1 (1973), 799-821.

[13] H. Ekblom and K. Madsen, Algorithms for non-linear Huber estimation, BIT., 29(1) (1989), 60-76.

[14] A. Guitton and W. S. William, Robust inversion of seismic data using the Huber norm, Geophys., 68(4) (2003), 1310-1319.

[15] H. Taeyoung, C. Wookeen, S. Changsoo, Waveform inversion using a back-propagation algorithm and a Huber function norm, Geophys., 74(3) (2009), R15-R24.

[16] X. Li, Z. L. Wang, Y. H. Chen and Q. L. Duan, Calculation of seismic curvature based on Huber norm, Oil Geophys. Prospect., 47(5) (2012), 758-765.

[17] Y. H. Wang, Multiple subtraction using an expanded multichannel matching filter, Geophys., 68(1) (2003), 346-354.

[18] D. J. Monk, Wave equation multiple suppression using constrained cross equalization, SEG Technical Program Expanded Abstract, (1991), 1309-1311.

[19] P. Li, Y. K. Liu, X. Chang, D. G. Jin, and S. S. Zhao, Application of the equipoise pseudo multichannel matching filter in multiple elimination using wave equation method, Chinese J. Geophys., 50(6) (2007), 1844-1853.

[20] H. F. Liu, Q. C. Li, and L. M. Wang, Suppression of multiples by improved expanding multichannel match minus method, Oil Geophys. Prospect., 44(3) (2009), 270-275.

[21] Y. T. Wu, Y. K. Liu, X. Chang, J. S. Zhang, B. S. Chen, P. Li, and X. C. Li, An improved matching method based on L1-norm for elimination and application in deep water basin of South China Sea, Chinese J. Geophys., 55(3) (2012), 1007-1016.

[22] Y. Shi, The practical method of predicting and suppressing multiple, Beijing, Chinese Academy of Sciences, 2010.

[23] Z. X. Zhou, Multiple elimination research based on feedback method. Dongying, China University of Petroleum, 2008.

[24] A. Guitton and D. J. Verschuur, Adaptive subtraction of multiples using $L1$-norm, Geophys. Prospect., 52(1) (2004), 27-38.

[25] H. L. Taylor and S. C. Banks, Deconvolution with the L-one norm,Geophys., (44) (1979), 39-52.

[26] A. Guitton, Huber solver versus IRLS algorithm for quasi $L1$ inversion, Stanford Explor. Project., 103 (2000), 205-266.

[27] F. J. Herrmann and D. J. Verschuur, Separation of primaries and multiples by non-linear estimation in the curvelet domain, 66rd annual international meeting, EAGE, Expanded Abstracts, (2004), 1953-1956.

[28] A. J. Candes and F. Guo, New multiscale transforms, minimum total variation synthesis: Applications to edge-preserving image reconstruction, Signal Process., 82 (2002), 1519-1543.